Fuel 316 (2022) 123255

Contents lists available at ScienceDirect

Fuel

journal homepage: www.elsevier.com/locate/fuel

Full Length Article

# Efficient dehydration of fructose into 5-HMF using a weakly-acidic catalyst prepared from a lignin-derived mesoporous carbon

Shuai Wang [a,b], Thomas L. Eberhardt [c], Hui Pan [a,b,*]

[a] Jiangsu Province Key Laboratory of Green Biomass-based Fuels and Chemicals, Nanjing 210037, China
[b] Jiangsu Co-Innovation Center of Efficient Processing and Utilization of Forest Resources, College of Chemical Engineering, Nanjing Forestry University, Nanjing 210037, China
[c] USDA Forest Service, Forest Products Laboratory, One Gifford Pinchot Drive, Madison, WI 53726, USA

ARTICLE INFO

*Keywords:*
Lignin
Weak acid
Mesoporous carbon
Fructose
5-HMF
Solid acid catalyst

ABSTRACT

A lignin-derived mesoporous carbon solid acid catalyst (LDMCC) was prepared using alkali lignin as a carbon source and KCl as a salt template to generate a carbon support that was carboxylated with acrylic acid. The prepared LDMCCs were characterized by various spectroscopies (FTIR, XPS, XRD, Raman), porosity determinations (BET), microscopies (SEM, TEM), thermogravimetric analysis, and acid-base titration. The LDMCC produced at the highest carbonization temperature (900 °C) possesses a rich porous structure, high specific surface area (1197.1 $m^2 \cdot g^{-1}$), large pore volume (0.63 $cm^3 \cdot g^{-1}$), and abundant –COOH groups (2.4 $mmol \cdot g^{-1}$). This weakly acidic catalyst exhibits excellent synergistic catalytic performance with DMSO in the catalytic dehydration of fructose to prepare 5-hydroxymethylfurfural (5-HMF); the yield of 5-HMF was 96.0% using dimethyl sulfoxide as the solvent, reaction conditions of 180 °C for 2.0 h, and a catalyst loading of 0.1 $mg \cdot mg^{-1}$. In addition, the prepared LDMCC exhibits excellent reusability over five cycles of use without significant loss in its catalytic activity. This study provides a novel green route for the preparation of a weakly acidic catalyst which may be useful for a variety of biomass conversion processes.

## 1. Introduction

As a renewable and versatile platform compound, 5-hydroxymethylfurural (5-HMF) can be employed as an intermediate to synthesize biofuels [1–3], such as 2,5-dimethylfuran [4] and 5-ethoxymethylfurfural [5], and high-value chemicals, such as levulinic acid [6] and 2,5-furandicarboxylic acid [7]. In recent years, 5-HMF has been obtained through the conversion of a series of renewable biomass-derived carbohydrates [8–10], such as fructose [11], glucose [12], sucrose [13], cellobiose [14], and cellulose [15]. The catalytic dehydration of fructose is considered to be a promising route to prepare 5-HMF with a high yield and under mild conditions [16,17].

Homogeneous catalytic systems have been widely applied to the dehydration of fructose to 5-HMF, with examples being ionic liquid [18], organic acid [19] and mineral acid [20] catalysts. Heterogeneous catalytic systems are gradually becoming more competitive, with examples being polymer [21], zeolite [22], metal oxide [23], heteropoly acid [24], functionalized silica [25], carbonaceous acid [26], and acidic ion-exchange resin [27] catalysts. Compared with the homogeneous catalyst systems, the heterogenous catalyst systems have advantages including ease of separation, excellent reusability, and lower corrosion [28,29]. Among the above-mentioned solid acid catalysts, cheaper carbonaceous acid catalysts prepared from lignin through carbonization and functionalization in succession have advantages of being both cost effective to produce and chemically stabile [30]. For example, Hu et al. [31] prepared a magnetic lignin-derived carbonaceous catalyst (MLC-$SO_3H$) through impregnation-carbonization-sulfonation using enzymatic hydrolysis lignin residue as a carbon source. Min et al. [32] synthesized a carbon solid acid (LCSA) with a high specific surface area derived from corncob lignin via simultaneous carbonization and activation followed by sulfonation. The prepared MLC-$SO_3H$ and LCSA catalysts were both applied to the catalytic dehydration of fructose to 5-HMF, and the 5-HMF yields of 81.1% and 75.7% can be obtained in dimethyl sulfoxide (DMSO), respectively. Although excellent catalytic effects can be achieved with sulfonated carbonaceous solid acid catalysts, the preparation of MLC-$SO_3H$ and LCSA required sulfonation with

* Corresponding author at: Jiangsu Co-Innovation Center of Efficient Processing and Utilization of Forest Resources, College of Chemical Engineering, Nanjing Forestry University, Nanjing 210037, China.
*E-mail address:* hpan@njfu.edu.cn (H. Pan).

https://doi.org/10.1016/j.fuel.2022.123255
Received 28 October 2021; Received in revised form 27 November 2021; Accepted 9 January 2022
Available online 29 January 2022

concentrated sulfuric acid that may raise equipment corrosion and environmental issues. Therefore, development of green and sustainable weakly acidic solid acids for biomass conversion is highly desired.

In addition to the catalyst, the reaction solvent plays an important role in 5-HMF production. Although water is the most environment-friendly solvent, the dehydration of fructose is generally non-selective when it is used as the reaction solvent. In order to improve the yield of 5-HMF, other reaction solvents, including γ-valerolactone (GVL) [33], tetrahydrofuran [34], ionic liquids [35], isopropyl alcohol [36], and DMSO [37] have been employed. Yang et al. [38] explored the effects of different solvents (i.e., N,N-dimethylformamide, n-butyl alcohol, ethylene glycol, toluene and DMSO) on the dehydration of fructose to 5-HMF. Among the solvents tested in their study, DMSO gave excellent performance for fructose dehydration to 5-HMF. Hu et al. [39] reported the impact of typical polar aprotic solvents (i.e., N-methylpyrrolidone (NMP), 4-methyl-2-pentanone (MIBK), 1,4-dioxane (DIO), GVL, THF and DMSO) on the degradative condensation of fructose. And the results revealed the distribution of the product in NMP or GVL (levulinic acid and oligomers), DIO or THF (formic acid and oligomers), MIBK (acetic acid and oligomers), and DMSO (5-HMF) in the initial stage of fructose conversion, indicating that DMSO is conducive to the formation of 5-HMF. In addition, DMSO demonstrated other advantages such as wide availability, low toxicity, and good solvency, which entitled it an excellent solvent for the dehydration of fructose to 5-HMF [40,41].

In the present study, a green, efficient, and simple strategy was employed to prepare a lignin-derived mesoporous carbon solid acid catalyst (LDMCC). An alkali lignin and KCl were used as a carbon source and a salt template, respectively, and the weakly-acidic catalysts generated using different carbonization temperatures followed by carboxylation with acrylic acid. The prepared LDMCCs were characterized by various spectroscopies (FTIR, XPS, XRD, Raman), porosity determinations (BET), microscopies (SEM, TEM), thermogravimetric analysis, and acid-base titration. The catalysts were then applied to the catalytic dehydration of fructose to 5-HMF to determine the effects of carbonization temperature, reaction solvent, catalyst loading, reaction temperature, reaction time, and the volume ratio of water to DMSO on the yield of 5-HMF. In addition, the reusability of the LDMCC was also studied under optimized fructose dehydration conditions.

## 2. Experimental

### 2.1. Materials

Alkali lignin, KCl and acrylic acid were purchased from Sigma-Aldrich, Nanjing Chemical Reagent Co., Ltd., and Aladdin Biochemical Technology Co., Ltd., respectively. Both fructose and DMSO were obtained from Sinopharm Chemical Reagent Co., Ltd.

### 2.2. Preparation of catalysts

Alkali lignin (2.0 g) and KCl (0.5 g) were thoroughly mixed with a mortar and pestle. The mixture was then transferred to a porcelain boat and carbonized in a high-temperature tube furnace in two stages with a constant flow of $N_2$ (60 mL/min): pre-carbonization stage (ramp 30 to 300 °C, 3 °C/min; hold at 300 °C for 1 h); high-temperature carbonization stage (ramp 300 to 700, 800, or 900 °C, 1 °C /min, hold at 700, 800, or 900 °C for 2 h). Carbonized products were washed with distilled water by vacuum filtration and dried at 80 °C to obtain the lignin-derived porous carbon (LDMC).

A given LDMC (1.0 g), acrylic acid (1.0 g) and of deionized water (8.0 mL) were added to a 25 mL hydrothermal reactor and then reacted at 190 °C for 16 h. The carboxylated product was vacuum filtered and washed with distilled water until the filtrate was neutral, and then dried at 80 °C to obtain the lignin-derived mesoporous carbon solid acid catalyst (LDMCC), labeled as LDMCC-700, LDMCC-800, and LDMCC-900 according to the 700, 800, and 900 °C carbonization temperature, respectively. Additionally, after five cycles of experiments, LDMCC-900 was labeled as LDMCC-900-R. And the schematic diagram of the preparation of the weakly acidic mesoporous carbon solid catalyst derived from lignin is shown in Fig. 1.

### 2.3. Characterization of catalysts

The surface chemistry was assessed using a Nicolet iS50 infrared spectrometer (4 $cm^{-1}$ resolution, 500 to 4000 $cm^{-1}$ spectral range). The $N_2$ adsorption–desorption isotherm was performed at − 196 °C on a Micromeritics ASAP 2020 physisorption analyzer. Before $N_2$ physisorption, degassing pretreatment was conducted at 100 °C for 6 h in a vacuum. Among them, the specific surface area and pore volume were calculated by the BET method, and the pore size distribution was calculated by the BJH model. The XRD pattern was measured on a X-2700 diffractometer (Cu Kα radiation, 5 ~ 80°, 10°/min). The microscopic morphology was observed using a FEI Tecnai G2 F20 transmission electron microscope (200 kV) and a JSM-7800F scanning electron microscope (10 kV). The thermal stability was measured on a Shimadzu DTG-60H thermogravimetric analyzer under $N_2$ atmosphere (30 to 800 °C, 10 °C/min). The Raman spectra were collected on a Renishaw inVia micro-Raman spectrometer (532 nm). The density of –COOH groups (mmol·$g^{-1}$) was measured by acid-base titration. First, 0.05 g of the catalyst was put into 20 mL $NaHCO_3$ aqueous solution (0.05 mol/L) and stirred at room temperature for 24 h. Then the catalyst was separated by filtration using a 0.22 μm aquo-system filter membrane, and the filtrate was titrated with 0.1 mol/L HCl aqueous solution. Among them, the pH value changes during the titration process were recorded by the OAKTON pH700 pH meter. The chemical bonding state and chemical element composition were recorded with a PerkinElmer PHI-1600 ESCA X-ray photoelectron spectroscope (Al Kα radiation).

### 2.4. Catalytic dehydration of fructose to 5-HMF

For the catalytic conversions, fructose (1.0 g), LDMCC (0.1 g), and DMSO (10 mL) were added to a 30 mL pressure tube and purged with $N_2$ atmosphere. The reaction mixture was reacted for 2 h at 180 °C under magnetic stirring (800 rpm). After the reaction, the pressure tube was quenched to room temperature and the spent LDMCC separated from the reaction mixture by filtration, washed with distilled water, dried at 80 °C overnight, and used for the next reaction. The reaction mixture contents of fructose and 5-HMF were determined by HPLC using an Agilent 1100 HPLC system equipped with an Aminex HPX-87H column and RI detector both maintained at 50 °C. Sulfuric acid aqueous solution (5 mM) was used as the mobile phase at a flow rate of 0.6 mL·$min^{-1}$. The fructose conversion and 5-HMF yield are calculated as follows:

$$\text{Fructose conversion } (\%) = \left(1 - \left(\frac{\text{Moles of fructose unreacted}}{\text{Moles of fructose added}}\right)\right) \times 100\%$$

$$\text{5-HMF yield } (\%) = \frac{\text{Moles of } 5-\text{HMF produced}}{\text{Moles of fructose added}} \times 100\%$$

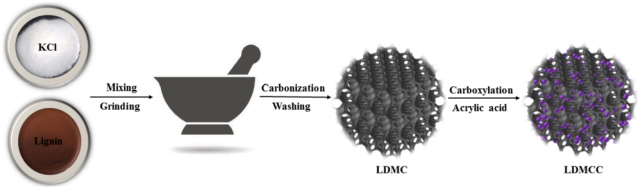


**Fig. 1.** Schematic diagram of preparation of weakly acidic mesoporous carbon solid catalyst derived from lignin.

## 3. Results and discussion

### 3.1. Structural characterization of catalysts

The FTIR spectra of the LDMCCs prepared with different carbonization temperatures are shown in Fig. 2. All three catalysts (LDMCC-700, LDMCC-800 and LDMCC-900) exhibited absorption peaks at 1100 $cm^{-1}$, 1710 $cm^{-1}$ and 3430 $cm^{-1}$, which are attributed to the vibrations of C-O, C=O and O–H, respectively [42–46]. Compared with the FTIR spectra of LDMC-900 support, it was found that the –COOH group was successfully introduced by the carboxylation with acrylic acid.

The XPS spectra of LDMCCs are shown in Fig. 3. In the full spectra (Fig. 3a, d, g), all the catalysts exhibited two main signals at 284.5 eV and 532.8 eV, corresponding to C 1 s and O 1 s, respectively [47]. The C 1 s spectra (Fig. 3b, e, h) could be fitted with three component peaks at 284.6 eV, 286.0 eV and 289.0 eV, which are assigned to C–C, C-O and C=O, respectively [48,49]. The O 1 s spectra (Fig. 3c, f, i) was only fitted with two component peaks at 532.0 eV and 533.4 eV, corresponding to C=O and C-O, respectively [50], consistent with the FTIR results.

The crystal structures of LDMCCs prepared with different carbonization temperatures were analyzed by XRD and Raman spectroscopy, and the results are shown in Fig. 4a and b, respectively. As seen from XRD patterns (Fig. 4a), all catalysts exhibited diffraction peaks centered at around 22° and 44°, with large widths and low intensities, which can be indexed to the (002) and (100) diffraction planes of graphite, respectively, suggesting the formation of the porous carbon with a limited degree of graphitization. In addition, two distinct peaks were observed at around 1340 $cm^{-1}$ (D-band) and 1590 $cm^{-1}$ (G-band) in the Raman spectra (Fig. 4b), which are attributed to disordered and graphitic carbon structure, respectively [51]. The intensity ratio of the D band to G band ($I_D/I_G$) reflects the degree of graphitization, and the lower ratio value means the higher degree of graphitization. The $I_D/I_G$ values of LDMCC-700, LDMCC-800 and LDMCC-900 are 1.65, 1.63 and 1.54, respectively, indicating that the degree of graphitization of the LDMCCs increased with the increasing carbonization temperature. Together, the XRD and Raman spectroscopy results indicate that LDMCCs exhibit a partial graphite structure.

The $N_2$ adsorption–desorption isotherms and pore size distributions of the LDMCCs are shown in Fig. 5a and 5b, respectively. As shown in Fig. 5a, all catalysts exhibited typical IV-type adsorption–desorption isotherms [52]. The sharp increase in $N_2$ adsorption at low relative pressure, and the presence of H4-type hysteresis loop at medium relative pressure, together indicate the co-existence of both microporous and mesoporous structures [53–56]. The pore size distribution of LDMCC-800 and LDMCC-900 were the same, concentrated around 4.0 nm (Fig. 5b); the result for LDMCC-700 was shifted to slightly smaller pore sizes.

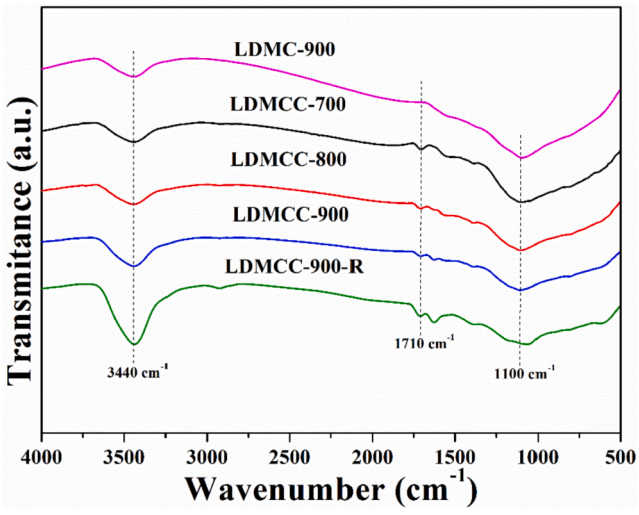


**Fig. 2.** FTIR spectra of catalysts prepared with different carbonization temperatures, LDMC-900 and LDMCC-900-R.

Differences in the textural parameters of the three LDMCCs are shown in Table 1. Here we see that the specific surface area and pore volume of the catalysts increased with the increase of carbonization temperature. The LDMCC-900 catalyst possesses the highest specific surface area (1197.1 $m^2 \cdot g^{-1}$) and pore volume (0.63 $cm^3 \cdot g^{-1}$) compared to the LDMCC-800 (1122.0 $m^2 \cdot g^{-1}$ and 0.59 $cm^3 \cdot g^{-1}$) and LDMCC-700 (829.7 $m^2 \cdot g^{-1}$ and 0.45 $cm^3 \cdot g^{-1}$). The above results indicate that the carbonization temperature has a significant effect on the structural characteristics of the lignin-derived mesoporous carbons, and those structural characteristics carry over to the textural parameters of the three catalysts.

The microstructure and morphology of the LDMCCs were observed by SEM and TEM (Fig. 6). As seen from SEM images (Fig. 6a ~ c), all the catalysts exhibited irregular morphology and rough surfaces with interconnected pores. The TEM images (Fig. 6d ~ f) show a rich porous structure, consistent with the SEM results. In addition, partial areas of slightly distorted graphene layers can be found in the high-resolution TEM images (Fig. 6g ~ i), indicating that a certain degree of graphitization occurred during the high-temperature carbonization process [57,58], which is consistent with the XRD and Raman spectroscopy results.

The thermal stability of the LDMCCs are shown in Fig. 7. All three catalysts exhibited a two-stage weight loss at approximately 100 °C and 250 °C. The slight weight loss in the first stage (0 ~ 100 °C) is mainly due to the loss of water. Compared with the TGA curve of LDMC-900 support, the significant weight loss in the second stage (200 ~ 300 °C) can be attributed to the decomposition of the –COOH groups. Here we see that thermal stability of the catalysts increases with increasing carbonization temperature. However, all the catalysts still appear to show sufficient thermal stability to be used for the catalytic dehydration of fructose to 5-HMF.

### 3.2. Catalytic performance of catalysts

#### 3.2.1. Effect of carbonization temperature

Reaction conditions: 1.0 g of fructose, 0.1 g of catalyst, 10 mL of DMSO, 140 °C for 2.0 h.

The catalytic performance of the LDMCCs for the dehydration of fructose to 5-HMF in DMSO was then investigated (Table 2) to assess the effect of the different carbonization temperatures used with the alkali lignin. As seen from Table 2, high fructose conversions of over 98.0% can be obtained using three catalysts prepared with different carbonization temperatures. With the increase in carbonization temperature for the LDMC used to prepare the catalyst, the yield of 5-HMF increased up to a maximum of 74.3% for LDMCC-900; yields of 68.3% and 58.7% were obtained for LDMCC-800 and LDMCC-700, respectively. Given that the yields coincide with specific surface area and pore volume data, we attribute the highest 5-HMF yield (74.3%), to the superior structural characteristics of LDMCC-900, those being the highest specific surface area (1197.1 $m^2 \cdot g^{-1}$), and largest pore volume (0.63 $cm^3 \cdot g^{-1}$), which are both beneficial to providing more catalytically active sites (2.4 $mmol \cdot g^{-1}$) [59].

#### 3.2.2. Effect of reaction solvent

Along with the selection of a catalyst with the appropriate functionality for the reaction being targeted, choosing a suitable reaction solvent for that particular catalyst is also a key factor to consider. The effect of the reaction solvent on the catalytic dehydration of fructose to 5-HMF was studied for the best performing catalyst (see Table 2), that being LDMCC-900. As shown in Fig. 8, for most of the investigated reaction solvents, at least half of the fructose was converted; the exception was with water where most of the fructose remained unreacted. A good

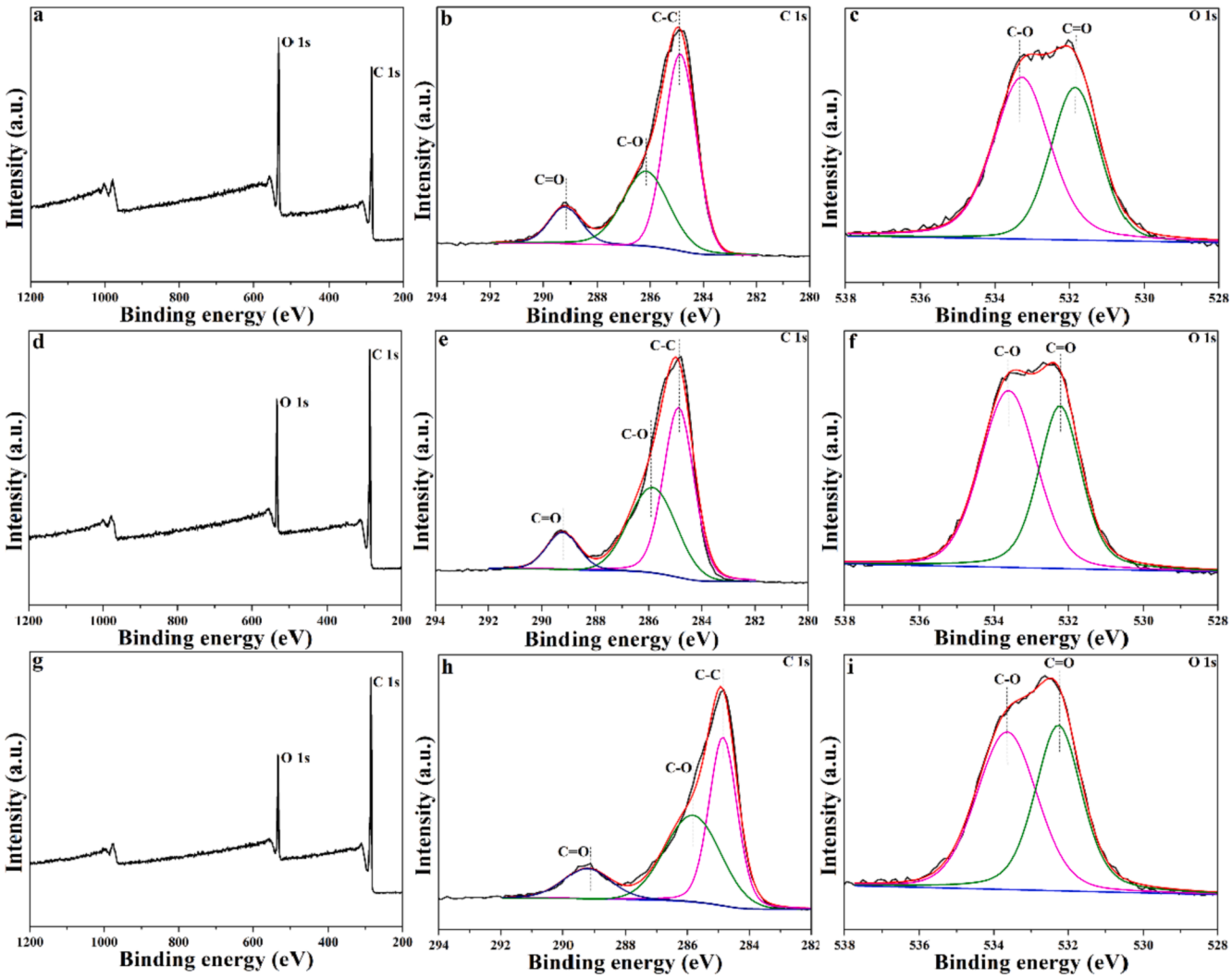


**Fig. 3.** XPS spectra of (a ~ c) LDMCC-700, (d ~ f) LDMCC-800 and (g ~ i) LDMCC-900.

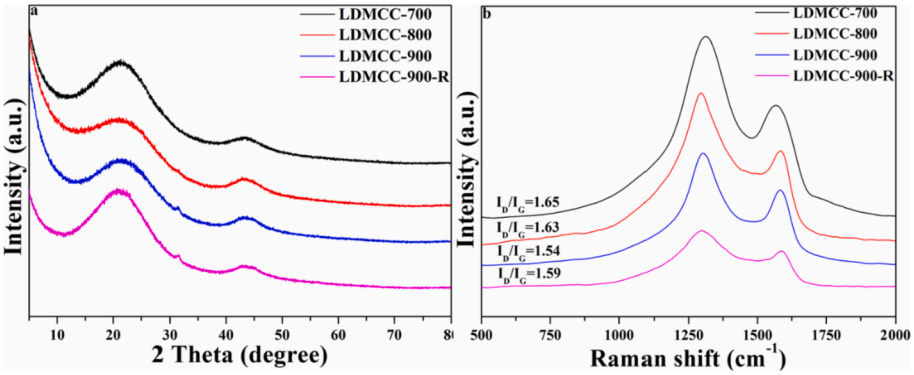


**Fig. 4.** (a) XRD patterns and (b) Raman spectra of catalysts prepared with different carbonization temperatures and LDMCC-900-R.

yield of 5-HMF (74.3%) was obtained with DMSO, but the yields of 5-HMF were less than 15.0% in all other reaction solvents ($H_2O$, ethanol, ethyl acetate, acetone and GVL). The higher yield with DMSO is attributed to the greater capacity of this solvent to inhibit the rehydration of 5-HMF into formic acid and levulinic acid by interacting with the water molecules produced by the reaction [60].

### 3.2.3. *Effect of catalyst loading*

Our screening of various reaction solvents established that DMSO is the most effective solvent of those evaluated for the dehydration of fructose to 5-HMF. The effect of catalyst loading on 5-HMF yield with DMSO as solvent was then investigated, with the results shown in Fig. 9. Even in the absence of catalyst, the conditions within the reaction system catalyzed the conversion of fructose to 5-HMF, with a conversion of 85.6%, but a yield of only 16.9%. When a small amount of LDMCC-900

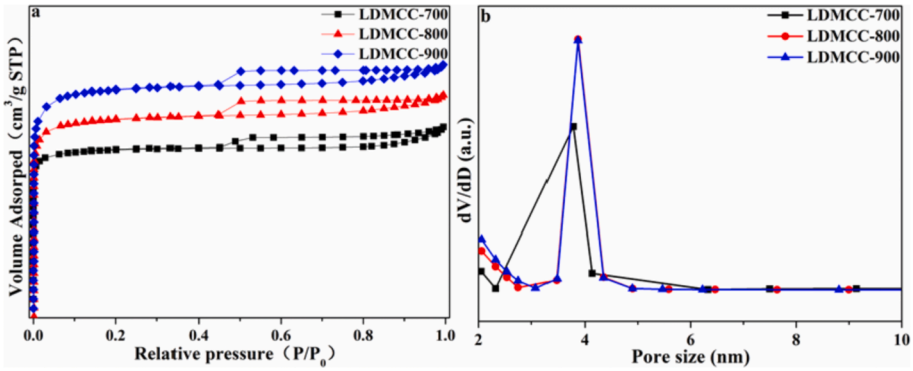


**Fig. 5.** (a) $N_2$ adsorption–desorption isotherms and (b) pore size distribution curves of catalysts prepared with different carbonization temperatures.

**Table 1**
Textural parameters (specific surface area, $S_{BET}$; pore volume, $V_{total}$) of catalysts prepared with different carbonization temperatures.

| Sample | $S_{BET}$ ($m^2 \cdot g^{-1}$) | $V_{total}$ ($cm^3 \cdot g^{-1}$) |
|---|---|---|
| LDMCC-700 | 829.7 | 0.45 |
| LDMCC-800 | 1122.0 | 0.59 |
| LDMCC-900 | 1197.1 | 0.63 |

catalyst (catalyst loading of 0.05 $mg \cdot mg^{-1}$) was added to the reaction system, the 5-HMF yield (50.9%) tripled, demonstrating its excellent catalytic performance in the dehydration of fructose to 5-HMF. With further increases of the catalyst loading, the 5-HMF yield gradually increased, and reached the maximum value of 74.3% at the catalyst loading of 0.1 $mg \cdot mg^{-1}$; this increase in 5-HMF yield is attributed to an increase of catalytic sites in the reaction system. Further increases in catalyst loading were of no benefit, suggesting a saturation of catalytic sites in the reaction system. Decreases in 5-HMF yield with catalyst

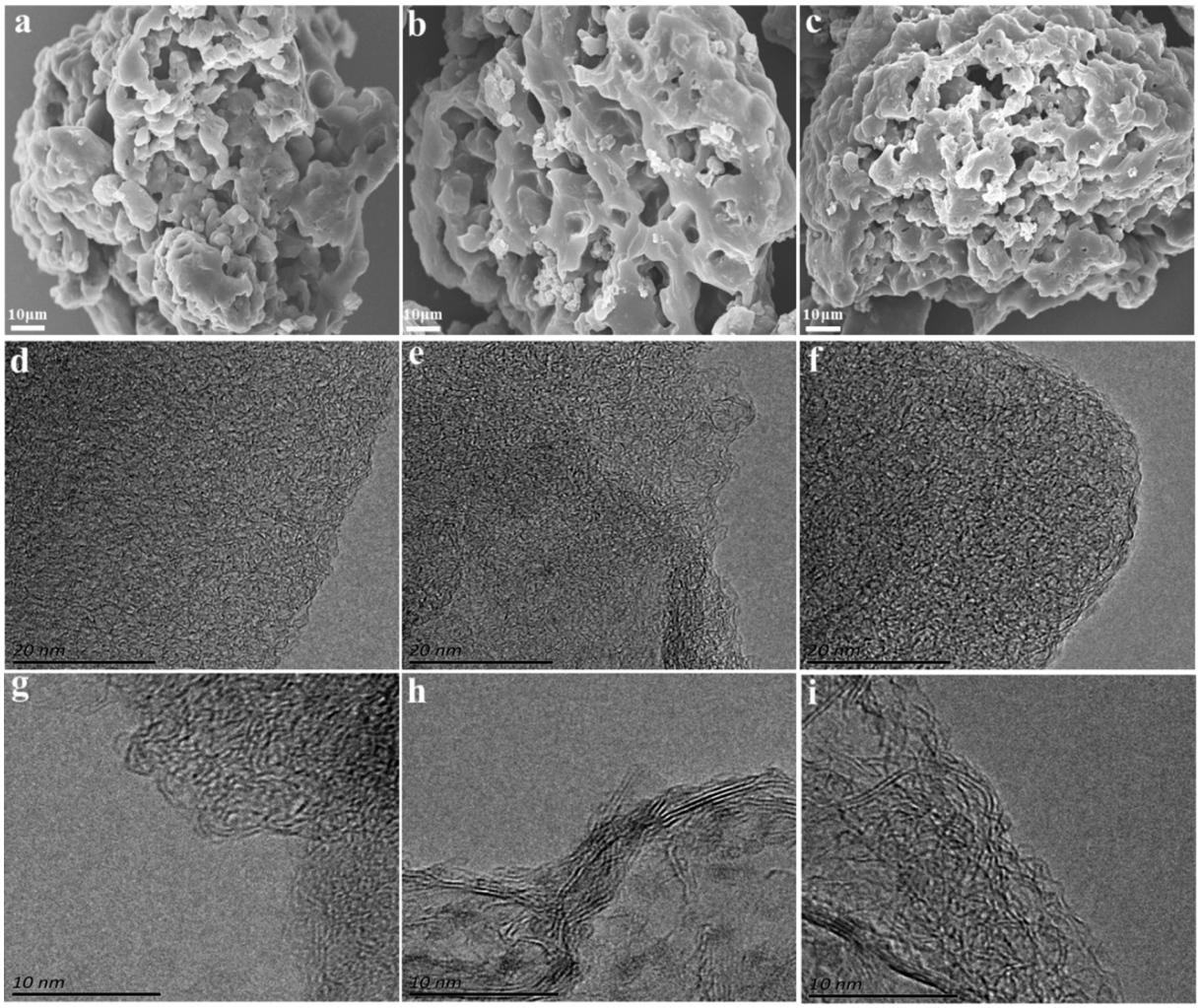


**Fig. 6.** SEM (a: LDMCC-700; b: LDMCC-800, and c: LDMCC-900), TEM (d: LDMCC-700; e: LDMCC-800, and f: LDMCC-900) and high-resolution TEM (g: LDMCC-700; h: LDMCC-800, and i: LDMCC-900) images of the LDMCC catalysts.

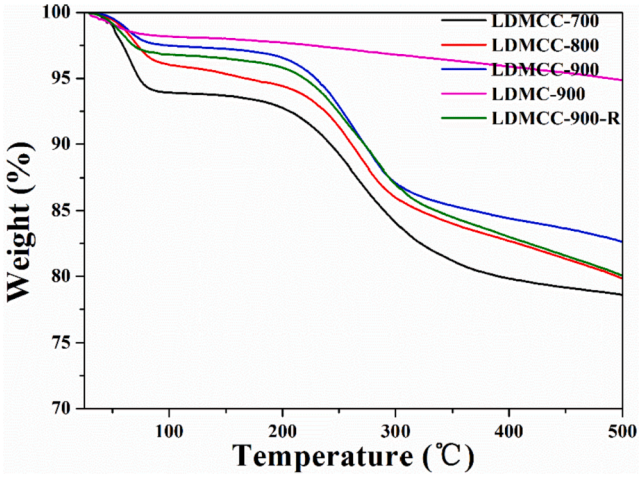


**Fig. 7.** TGA curves of catalysts prepared with different carbonization temperatures, LDMC-900 and LDMCC-900-R.

**Table 2**
The effect of carbonization temperature on fructose conversion and 5-HMF yield.

| Catalyst | Fructose conversion (%) | 5-HMF yield (%) | –COOH density (mmol·g$^{-1}$) |
|---|---|---|---|
| LDMCC-700 | 99.3 | 58.7 | 2.0 |
| LDMCC-800 | 99.5 | 68.3 | 2.0 |
| LDMCC-900 | 98.9 | 74.3 | 2.4 |

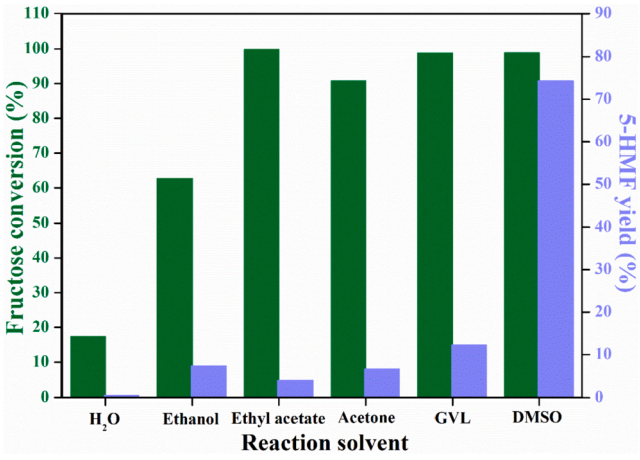


**Fig. 8.** The effect of reaction solvent on fructose conversion and 5-HMF yield. Reaction conditions: 1.0 g of fructose, 0.1 g of LDMCC-900 catalyst, 10 mL of reaction solvent, 140 °C for 2.0 h.

loadings above 0.1 mg·mg$^{-1}$ were extremely minor but could suggest that the solid catalyst, when present in excessive amounts, could result in the rehydration of 5-HMF to form other by-products such as formic acid and levulinic acid [61].

### 3.2.4. Effects of reaction temperature and reaction time

Given the results from the catalyst loading experiment, a catalyst loading of 0.1 mg·mg$^{-1}$ was selected as optimal and used in our subsequent experiments. Next, we determined the effects of reaction temperature and reaction time on 5-HMF yields. Fig. 10a shows that when the reaction temperature of 120 °C was used, the 5-HMF yield and

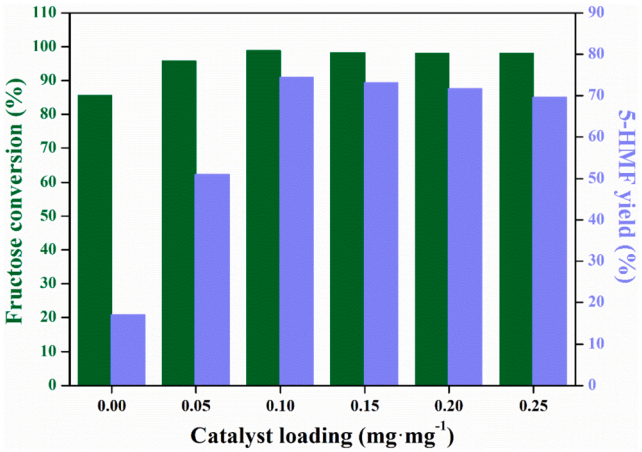


**Fig. 9.** The effect of catalyst loading on fructose conversion and 5-HMF yield. Reaction conditions: 1.0 g of fructose, 10 mL of DMSO, 140 °C for 2.0 h.

fructose conversion were 73.1% and 52.4%, respectively. With increasing reaction temperature, from 120 °C to 180 °C, the fructose was completely converted, and the yield of 5-HMF increased to a maximum of 96.0%. The literature shows that DMSO begins to slowly decompose around its boiling temperature (189 °C) [62]. To further explore the role of DMSO in the catalytic dehydration of fructose to 5-HMF, additional reactions without adding catalyst were carried out at three temperatures (140 °C, 160 °C and 180 °C) and the results were compared with those in the presence of catalyst LDMCC-900 as shown in Table S1. It can be seen from Table S1 that high fructose conversions were achieved at relatively low temperature of 140 °C (around 85.0%) in the absence of catalyst, indicating the catalytic effect of DMSO with fructose conversion. However, only 16.9%, 26.1% and 33.6% of 5-HMF yields were obtained under 140 °C, 160 °C and 180 °C, respectively. Noteworthy, when a small amount (0.1 g) of LDMCC-900 catalyst was added to the reaction system, the yields of 5-HMF increased dramatically to 74.3%, 84.8% and 96.0%, respectively, under the same reaction conditions, which fully demonstrated the excellent catalysis performance of LDMCC-900. Therefore, it can be concluded that the high yield of 5-HMF from the dehydration of fructose catalyzed by LDMCC-900 in DMSO can be attributed to the synergistic effect of the catalyst (LDMCC-900) and the solvent (DMSO). Back to Fig. 10a, increasing the reaction temperature just 10 °C more, to 190 °C, resulted in the yield of 5-HMF to drop to 84.9%. Given that the color of the reaction mixture changed to dark brown or black with this 10°increase in temperature, thermal degradation of the reaction product seemingly accelerated, resulting in undesirable side reactions such as the polymerization or cross-polymerization of 5-HMF and/or fructose into humins [63,64].

Regarding the effects of reaction time (Fig. 10b), essentially all fructose was converted with reaction times ranging from 0.5 to 3 h. For the yield of 5-HMF, that gradually increased with longer reaction times, reaching the maximum value (96.5%) at a reaction time of 2.5 h; lower 5-HMF yields observed with shorter reaction times have shown the presence of partially dehydrated intermediates [59]. As the reaction time further increased to 3.0 h, the yield of 5-HMF decreased to 88.3%, likely because excessive reaction time caused the occurrence of undesirable side reactions, such as the rehydration of 5-HMF to levulinic acid and formic acid [65]. Considering the economic and actual needs, the reaction temperature and reaction time of 180 °C and 2.0 h, respectively, were selected as the optimal reaction conditions for the dehydration of fructose to 5-HMF (fructose conversion of 100% and 5-HMF yield of 96.0%).

### 3.2.5. Effect of volume ratio of water to DMSO

As a dehydration reaction, the addition of water in the solvent system should significantly affect the catalytic performance of the LDMCC-900.

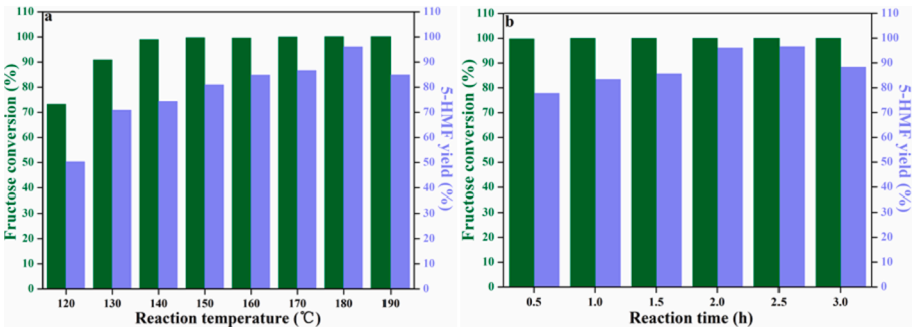


**Fig. 10.** The effects of (a) reaction temperature and (b) reaction time on fructose conversion and 5-HMF yield. Reaction conditions: (a) 1.0 g of fructose, 0.1 g of LDMCC-900, 10 mL of DMSO, 2.0 h; (b) 1.0 g of fructose, 0.1 g of LDMCC-900, 10 mL of DMSO, 180 °C.

The effect of the volume ratio of water to DMSO on 5-HMF yield was investigated by 6 different solvent ratios as shown in Fig. 11. In the presence of the LDMCC-900, the fructose conversion of up to 87.2% could be obtained, while the 5-HMF yield was only 42.4% with water alone as the reaction solvent. This is mainly due to the instability of 5-HMF, which is easily rehydrated to form formic acid levulinic acid; also, 5-HMF can cross-link to form humins at a high temperature [66]. With the increase of DMSO content in the solvent system, the yield of 5-HMF gradually increased and reached the maximum value of 96.0% in pure DMSO, demonstrating a that stepwise additions of water impart a stepwise reduction in the yield of 5-HMF.

### 3.2.6. *Reusability of catalysts*

In addition to catalytic activity, the reusability of the catalyst is another important aspect of its catalytic performance. To study the reusability of LDMCC-900 in the catalytic dehydration of fructose to 5-HMF in DMSO, five cycles of experiments were carried out (Fig. 12). After the fifth cycle, a 5-HMF yield of 89.5% could still be maintained. The density of the –COOH groups on LDMCC-900-R was 2.2 mmol·g$^{-1}$ also measured by acid-base titration. Compared with LDMCC-900 (2.4 mmol·g$^{-1}$), the density of –COOH groups on LDMCC-900-R decreased slightly after five reaction cycles. The slight decrease in 5-HMF yield may be attributed to the loss of –COOH groups and the deposition of polymer by-products on LDMCC-900 during the dehydration process [67]. In addition, the additional recycling experiments were carried out under milder reaction conditions (1.0 g fructose, 0.1 g catalyst, 10 mL DMSO, 120 °C for 2.0 h) and consequently, lower conversion and yields were observed than those at optimized reaction conditions. The results are listed in Fig. S1. It can be seen that at lower fructose conversion and

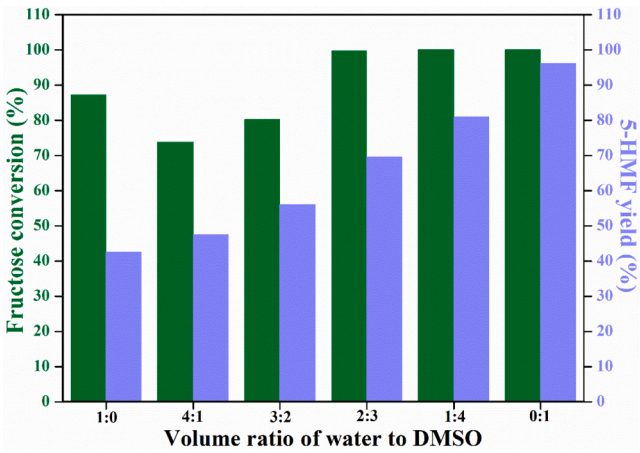


**Fig. 11.** The effect of volume ratio of water to DMSO on fructose conversion and 5-HMF yield. Reaction conditions: 1.0 g of fructose, 0.1 g of LDMCC-900 catalyst, 10 mL of reaction solvent, 180 °C for 2.0 h.

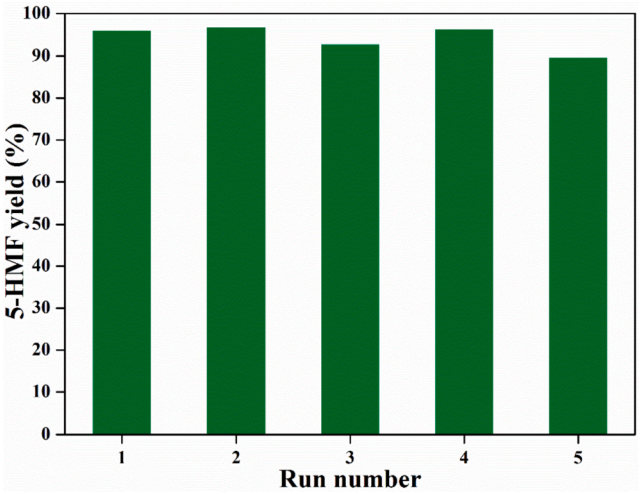


**Fig. 12.** Catalyst reusability in the dehydration of fructose to 5-HMF. Reaction conditions: 1.0 g of fructose, 0.1 g of LDMCC-900, 10 mL of DMSO, 180 °C for 2.0 h.

5-HMF yield, the catalyst LDMCC-900 only provided slightly decreased catalytic activity, indicating that LDMCC-900 has excellent reusability. The excellent reusability of LDMCC-900 demonstrates its potential as a green and sustainable catalyst for the dehydration of fructose to 5-HMF in DMSO.

To further explore the changes of the LDMCC-900 catalyst after five cycles of experiments, recovered catalyst LDMCC-900-R was characterized with FTIR, XRD, Raman, SEM and TGA. The results were compared with those of the fresh prepared catalyst LDMCC-90. The FTIR spectra (Fig. 2) and SEM image (Fig. S2) of LDMCC-900-R confirm that the surface functional groups and porous carbon framework of LDMCC-900 did not undergo obvious changes after the recycling experiments. Nevertheless, as depicted in the XRD (Fig. 4a), the peak intensity at 22° assigned for the (0 0 2) plane of amorphous carbon in LDMCC-900-R increased slightly, indicating the decrease in the degree of graphitization after the recycling experiments. The Raman result (Fig. 4b) shows that the $I_D/I_G$ value (1.59) is slightly higher than that of LDMCC-900, which is in agreement of the XRD results. This result should be attributed to the increase of defects in the structure of LDMCC-900-R during the recycling experiments. Noteworthy, the TGA curve (Fig. 7) of LDMCC-900-R suggests that although the thermal stability of recovered catalyst is slightly lower than that of fresh prepared catalyst, it still shows sufficient thermal stability for the catalytic dehydration of fructose to 5-HMF.

## 4. Conclusions

A series of LDMCCs was prepared using alkali lignin as the carbon source and KCl as the salt template to generate a carbon supports at different carbonization temperatures that were then carboxylated with acrylic acid. The prepared LDMCC-900 has excellent structural characteristics such as high specific surface area, large pore volume and sufficient –COOH groups, and exhibits excellent synergistic catalytic performance with DMSO in the catalytic dehydration of fructose to 5-HMF. A 5-HMF yield of 96.0% was obtained in DMSO at 180 °C for 2.0 h with a LDMCC-900 loading of 0.1 mg·mg$^{-1}$. Moreover, no significant decrease in catalytic activity was observed after five cycles of LDMCC-900 use, indicating that it has good reusability. Compared with sulfonated solid acid catalyst reported in the literature, the catalytic performance of the LDMCC-900 for the dehydration of fructose to 5-HMF is comparable in terms of yield although a slightly higher reaction temperature may be required. More importantly, the preparation process of LDMCC is greener than sulfonated solid acids, mainly because the former is simply functionalized with acrylic acid, while the latter generally require concentrated sulfuric acid for the sulfonation.

### *CRediT authorship contribution statement*

**Shuai Wang:** Investigation, Writing – original draft. **Thomas L. Eberhardt:** Supervision, Writing – review & editing. **Hui Pan:** Conceptualization, Supervision, Writing – review & editing.

### Declaration of Competing Interest

The authors declare that they have no known competing financial interests or personal relationships that could have appeared to influence the work reported in this paper.

### Acknowledgements

The authors are grateful for the financial support from National Natural Science Foundation of China (No. 31770631) and National Key Basic Research Program of China (2017YFD0601005).

### Appendix A. Supplementary data

Supplementary data to this article can be found online at https://doi.org/10.1016/j.fuel.2022.123255.

### References

[1] Bai C, Hou Q, Bai X, Nie Y, Qian H, Zhen M, et al. Conversion of glucose to 5-hydroxymethylfurfural at high substrate loading: effect of catalyst and solvent on the stability of 5-hydroxymethylfurfural. Energ Fuel 2020;34(12):16240–9.
[2] Hou Q, Zhen M, Li W, Liu L, Liu J, Zhang S, et al. Efficient catalytic conversion of glucose into 5-hydroxymethylfurfural by aluminum oxide in ionic liquid. Appl Catal B-Environ 2019;253:1–10.
[3] Hou Q, Zhen M, Liu L, Chen Y, Huang F, Zhang S, et al. Tin phosphate as a heterogeneous catalyst for efficient dehydration of glucose into 5-hydroxymethylfurfural in ionic liquid. Appl Catal B-Environ 2018;224:183–93.
[4] Wang H, Zhu C, Li D, Liu Q, Tan J, Wang C, et al. Recent advances in catalytic conversion of biomass to 5-hydroxymethylfurfural and 2, 5-dimethylfuran. Renew Sust Energ Rev 2019;103:227–47.
[5] Li H, Saravanamurugan S, Yang S, Riisager A. Direct transformation of carbohydrates to the biofuel 5-ethoxymethylfurfural by solid acid catalysts. Green Chem 2016;18(3):726–34.
[6] Garcés D, Díaz E, Ordóñez S. Aqueous phase conversion of hexoses into 5-hydroxymethylfurfural and levulinic acid in the presence of hydrochloric acid: mechanism and kinetics. Ind Eng Chem Res 2017;56(18):5221–30.
[7] Xu S, Zhou P, Zhang Z, Yang C, Zhang B, Deng K, et al. Selective oxidation of 5-hydroxymethylfurfural to 2, 5-furandicarboxylic acid using $O_2$ and a photocatalyst of Co-thioporphyrazine bonded to g-$C_3N_4$. J Am Chem Soc 2017;139(41):14775–82.
[8] Hou Q, Qi X, Zhen M, Qian H, Nie Y, Bai C, et al. Biorefinery roadmap based on catalytic production and upgrading 5-hydroxymethylfurfural. Green Chem 2021;23(1):119–231.
[9] Nie Y, Hou Q, Bai C, Qian H, Bai X, Ju M. Transformation of carbohydrates to 5-hydroxymethylfurfural with high efficiency by tandem catalysis. J Clean Prod 2020;274:123023. https://doi.org/10.1016/j.jclepro.2020.123023.
[10] Hou Q, Li W, Zhen M, Liu L, Chen Y, Yang Q, et al. An ionic liquid-organic solvent biphasic system for efficient production of 5-hydroxymethylfurfural from carbohydrates at high concentrations. RSC Adv 2017;7(75):47288–96.
[11] Karimi S, Seidi F, Niakan M, Shekaari H, Masteri-Farahani M. Catalytic dehydration of fructose into 5-hydroxymethylfurfural by propyl sulfonic acid functionalized magnetic graphene oxide nanocomposite. Renew Energ 2021;180:132–9.
[12] Rezayan A, Wang K, Nie R, Lu T, Wang J, Zhang Y, et al. Synthesis of bifunctional tin-based silica-carbon catalysts, Sn/KIT-1/C, with tunable acid sites for the catalytic transformation of glucose into 5-hydroxymethylfurfural. Chem Eng J 2022;429:132261. https://doi.org/10.1016/j.cej.2021.132261.
[13] Tian XT, Qi BK, Zhang SF, Luo JQ, Wan YH. Catalytic production of 5-hydroxymethylfurfural from sucrose and molasses by aluminum chloride in green aqueous γ-valerolactone system. Biomass Convers Bior 2020;11:1–11.
[14] Qi T, Si Z-B, Liu L-J, Yang H-M, Huang Z, Yang H-Q, et al. Mechanistic study of cellobiose conversion to 5-hydroxymethylfurfural catalyzed by a Brønsted acid with counteranions in an aqueous solution. Phys Chem Chem Phys 2020;22(17):9349–61.
[15] Fang J, Zheng W, Liu K, Li H, Li C. Molecular design and experimental study on the synergistic catalysis of cellulose into 5-hydroxymethylfurfural with Brønsted-Lewis acidic ionic liquids. Chem Eng J 2020;385:123796. https://doi.org/10.1016/j.cej.2019.123796.
[16] Deshan ADK, Forero JJ, Bartley JP, Marasinghege C, Tuiatua K, Beltramini J, et al. Structural features of cotton gin trash derived carbon material as a catalyst for the dehydration of fructose to 5-hydroxymethylfurfural. Fuel 2021;306:121670. https://doi.org/10.1016/j.fuel.2021.121670.
[17] Wang J, Zhang Z, Jin S, Shen X. Efficient conversion of carbohydrates into 5-hydroxylmethylfurfan and 5-ethoxymethylfurfural over sufonic acid-functionalized mesoporous carbon catalyst. Fuel 2017;192:102–7.
[18] Ma H, Zhou B, Li YQ, Argyropoulos DS. Conversion of fructose to 5-hydroxymethylfurfural with a functionalized ionic liquid. BioResources 2012;7:533–44.
[19] Jiang N, Huang R, Qi W, Su R, He Z. Effect of formic acid on conversion of fructose to 5-hydroxymethylfurfural in aqueous/butanol media. BioEnergy Res 2012;5(2):380–6.
[20] Bicker M, Hirth J, Vogel H. Dehydration of fructose to 5-hydroxymethylfurfural in sub-and supercritical acetone. Green Chem 2003;5(2):280–4.
[21] Du M, Agrawal AM, Chakraborty S, Garibay SJ, Limvorapitux R, Choi B, et al. Matching the activity of homogeneous sulfonic acids: The fructose-to-HMF conversion catalyzed by hierarchically porous sulfonic-acid-functionalized porous organic polymer (POP) catalysts. ACS Sustain Chem Eng 2019;7(9):8126–35.
[22] Ma ZS, Hu HL, Sun ZQ, Fang WT, Zhang J, Yang LF, et al. Acidic zeolite L as a highly efficient catalyst for dehydration of fructose to 5-hydroxymethylfurfural in ionic liquid. ChemSusChem 2017;10:1669–74.
[23] García-López EI, Pomilla FR, Megna B, Testa ML, Liotta LF, Marcì G. Catalytic dehydration of fructose to 5-hydroxymethylfurfural in aqueous medium over $Nb_2O_5$-based catalysts. Nanomaterials 2021;11(7):1821. https://doi.org/10.3390/nano11071821.
[24] Ganji P. Synthesis and catalytic performance of $Sn_x$STA by microwave-assisted hydrothermal synthesis for fructose to HMF. Biomass Convers Bior 2020;10(4):823–30.
[25] Wang L, Zhang L, Li H, Ma Y, Zhang R. High selective production of 5-hydroxymethylfurfural from fructose by sulfonic acid functionalized SBA-15 catalyst. Compos Part B-Eng 2019;156:88–94.
[26] He Q, Lu YC, Peng Q, Chen WH, Fan GZ, Chai B, et al. Synthesis of 5-hydroxymethylfurfural from fructose catalyzed by sulfonated carbon-based solid acid. Biomass Convers Bior 2021:1–9.
[27] Aellig C, Hermans I. Continuous D-fructose dehydration to 5-hydroxymethylfurfural under mild conditions. ChemSusChem 2012;5(9):1737–42.
[28] Li Y, Liu H, Song C, Gu X, Li H, Zhu W, et al. The dehydration of fructose to 5-hydroxymethylfurfural efficiently catalyzed by acidic ion-exchange resin in ionic liquid. Bioresource Technol 2013;133:347–53.
[29] Hafizi H, Najafi Chermahini A, Saraji M, Mohammadnezhad G. The catalytic conversion of fructose into 5-hydroxymethylfurfural over acid-functionalized KIT-6, an ordered mesoporous silica. Chem Eng J 2016;294:380–8.
[30] Gan L, Lyu Li, Shen T, Wang S. Sulfonated lignin-derived ordered mesoporous carbon with highly selective and recyclable catalysis for the conversion of fructose into 5-hydroxymethylfurfural. Appl Catal A-Gen 2019;574:132–43.
[31] Hu L, Tang X, Wu Z, Lin L, Xu J, Xu N, et al. Magnetic lignin-derived carbonaceous catalyst for the dehydration of fructose into 5-hydroxymethylfurfural in dimethylsulfoxide. Chem Eng J 2015;263:299–308.
[32] Li M, Zhang Q, Luo B, Chen C, Wang S, Min D. Lignin-based carbon solid acid catalyst prepared for selectively converting fructose to 5-hydroxymethylfurfural. Ind Crop Prod 2020;145:111920. https://doi.org/10.1016/j.indcrop.2019.111920.
[33] Qi L, Mui YF, Lo SW, Lui MY, Akien GR, Horváth IT. Catalytic conversion of fructose, glucose, and sucrose to 5-(hydroxymethyl)furfural and levulinic and formic acids in γ-valerolactone as a green solvent. ACS Catal 2014;4(5):1470–7.
[34] Gallo JMR, Alamillo R, Dumesic JA. Acid-functionalized mesoporous carbons for the continuous production of 5-hydroxymethylfurfural. J Mol Catal A-Chem 2016;422:13–7.
[35] Li C, Zhao ZK, Cai H, Wang A, Zhang T. Microwave-promoted conversion of concentrated fructose into 5-hydroxymethylfurfural in ionic liquids in the absence of catalysts. Biomass Bioenerg 2011;35(5):2013–7.

[36] Pawar H, Lali A. DICAT-2: Solid acid catalyst with a protagonist backbone for microwave assisted synthesis of 5-hydroxymethylfurfural in isopropyl alcohol. Ind Eng Chem Res 2018;57(43):14428–39.
[37] Mantovani M, Mandelli D, Gonçalves M, Carvalho WA. Fructose dehydration promoted by acidic catalysts obtained from biodiesel waste. Chem Eng J 2018;348:860–9.
[38] Zhao J, Zhou C, He C, Dai Y, Jia X, Yang Y. Efficient dehydration of fructose to 5-hydroxymethylfurfural over sulfonated carbon sphere solid acid catalysts. Catal Today 2016;264:123–30.
[39] Fu X, Hu Y, Zhang Y, Zhang Y, Tang D, Zhu L, et al. Solvent effects on degradative condensation side reactions of fructose in its initial conversion to 5-hydroxymethylfurfural. ChemSusChem 2020;13(3):501–12.
[40] Kimura H, Nakahara M, Matubayasi N. Solvent effect on pathways and mechanisms for D-fructose conversion to 5-hydroxymethyl-2-furaldehyde: In situ $^{13}C$ NMR study. J Phys Chem A 2013;117:2102–13.
[41] Nunes RS, Reis GM, Vieira LM, Mandelli D, Carvalho WA. Ultra-fast selective fructose dehydration promoted by a kraft lignin sulfonated carbon under microwave heating. Catal Lett 2021;151(2):398–408.
[42] Song W, Zhang Y, Varyambath A, Kim JS, Kim I. Sulfonic acid modified hollow polymer nanospheres with tunable wall-thickness for improving biodiesel synthesis efficiency. Green Chem 2020;22(11):3572–83.
[43] Shen S, Cai B, Wang C, Li H, Dai G, Qin H. Preparation of a novel carbon-based solid acid from cocarbonized starch and polyvinyl chloride for cellulose hydrolysis. Appl Catal A-Gen 2014;473:70–4.
[44] Shim SH, Kim KT, Lee JU, Jo WH. Facile method to functionalize graphene oxide and its application to poly (ethylene terephthalate)/graphene composite. ACS Appl Mater Inter 2012;4(8):4184–91.
[45] Cai X-M, Chen X, Chen X, Li Y, Wang F. A luminescent cellulose ether with a regenerated crystal form obtained in tetra(n-butyl)ammonium hydroxide/dimethyl sulfoxide. Carbohyd Polym 2020;230:115649. https://doi.org/10.1016/j.carbpol.2019.115649.
[46] Cai XM, Lin YT, Chen XF, Chen X, Mu TQ, Huang SL, et al. Linker regulation: Synthesis and electrochemical properties of ferrocene-decorated cellulose. J Inorg Organomet P 2020;30:3771-80.
[47] Li J, Wei L, Jiang Q, Liu C, Zhong L, Wang X. Salt-template assisted synthesis of cornstalk derived hierarchical porous carbon with excellent supercapacitance. Ind Crop Prod 2020;154:112666. https://doi.org/10.1016/j.indcrop.2020.112666.
[48] Zhong Y, Deng Q, Yao Q, Lu C, Zhang P, Li H, et al. Functionalized biochar with superacidity and hydrophobicity as a highly efficient catalyst in the synthesis of renewable high-density fuels. ACS Sustain Chem Eng 2020;8(21):7785–94.
[49] Li Q, Hu M, Wang K, Wang X. One-step approach for fabrication of 3D porous carbon/graphene composites as supercapacitor electrode materials. Catal Today 2019;330:228–39.
[50] Wang C, Wu D, Wang H, Gao Z, Xu F, Jiang K. A green and scalable route to yield porous carbon sheets from biomass for supercapacitors with high capacity. J Mater Chem A 2018;6(3):1244–54.
[51] Sun L, Zhou Y, Li L, Zhou H, Liu X, Zhang Q, et al. Facile and green synthesis of 3D honeycomb-like N/S-codoped hierarchically porous carbon materials from bio-protic salt for flexible, temperature-resistant supercapacitors. Appl Surf Sci 2019;467-468:382–90.
[52] Liu B, Ren Y, Zhang Z. Aerobic oxidation of 5-hydroxymethylfurfural into 2, 5-furandicarboxylic acid in water under mild conditions. Green Chem 2015;17(3):1610–7.
[53] Li J, Xiao R, Li M, Zhang H, Wu S, Xia C. Template-synthesized hierarchical porous carbons from bio-oil with high performance for supercapacitor electrodes. Fuel Process Technol 2019;192:239–49.
[54] Yan T, Wan Z, Wang K, Hu M, Wang X. A 3D carbon foam derived from phenol resin via CsCl soft-templating approach for high-performance supercapacitor. Energy Technol 2020;8(3):1901301. https://doi.org/10.1002/ente.v8.310.1002/ente.201901301.
[55] Cui Y, Liu W, Lyu Y, Zhang Y, Wang H, Liu Y, et al. All-carbon lithium capacitor based on salt crystal-templated, N-doped porous carbon electrodes with superior energy storage. J Mater Chem A 2018;6(37):18276–85.
[56] Ouyang T, Cheng K, Gao Y, Kong S, Ye K, Wang G, et al. Molten salt synthesis of nitrogen doped porous carbon: a new preparation methodology for high-volumetric capacitance electrode materials. J Mater Chem A 2016;4(25):9832–43.
[57] Xing B, Zhang C, Liu Q, Zhang C, Huang G, Guo H, et al. Green synthesis of porous graphitic carbons from coal tar pitch templated by nano-$CaCO_3$ for high-performance lithium-ion batteries. J. Alloy Compd 2019;795:91–102.
[58] Li Y, Shen J, Li J, Sun X, Shen J, Han W, et al. A protic salt-derived porous carbon for efficient capacitive deionization: Balance between porous structure and chemical composition. Carbon 2017;116:21–32.
[59] Zhang S, Zheng Z, Zhao C, Zhang L. Fabrication of a novel and high-performance mesoporous ethylene tar-based solid acid catalyst for the dehydration of fructose into 5-hydroxymethylfurfural. ACS Omega 2017;2(9):6123–30.
[60] Aljammal N, Lenssens A, Reviere A, Verberckmoes A, Thybaut JW, Verpoort F, et al. Metal–organic frameworks as catalysts for fructose conversion into 5-hydroxymethylfurfural: catalyst screening and parametric study. Appl Organomet Chem 2021;35(12). https://doi.org/10.1002/aoc.v35.1210.1002/aoc.6419.
[61] Mukherjee A, Dumont M-J, Raghavan V. Sustainable production of hydroxymethylfurfural and levulinic acid: challenges and opportunities. Biomass Bioenergy 2015;72:143–83.
[62] Deguchi Y, Kono M, Koizumi Y, Izato Y-I, Miyake A. Study on autocatalytic decomposition of dimethyl sulfoxide (DMSO). Org Process Res Dev 2020;24(9):1614–20.
[63] Tomer R, Biswas P. Dehydration of glucose/fructose to 5-hydroxymethylfurfural (5-HMF) over an easily recyclable sulfated titania ($SO_4^{2-}/TiO_2$) catalyst. New J Chem 2020;44(47):20734–50.
[64] Cai H, Li C, Wang A, Xu G, Zhang T. Zeolite-promoted hydrolysis of cellulose in ionic liquid, insight into the mutual behavior of zeolite, cellulose and ionic liquid. Appl Catal B-Environ 2012;123-124:333–8.
[65] Jin P, Zhang Y, Chen Y, Pan J, Dai X, Liu M, et al. Facile synthesis of hierarchical porous catalysts for enhanced conversion of fructose to 5-hydroxymethylfurfural. J Taiwan Inst Chem Eng 2017;75:59–69.
[66] Sun S, Zhao L, Yang J, Wang X, Qin X, Qi X, et al. Eco-friendly synthesis of $SO_3H$-containing solid acid via mechanochemistry for the conversion of carbohydrates to 5-hydroxymethylfurfural. ACS Sustain Chem Eng 2020;8(18):7059–67.
[67] Zhang T, Li W, Jin Y, Ou W. Synthesis of sulfonated chitosan-derived carbon-based catalysts and their applications in the production of 5-hydroxymethylfurfural. Int J Biol Macromol 2020;157:368–76.